Geometry of random potentials: Induction of 2D gravity in Quantum Hall plateau transitions

Riccardo Conti,[1] Hrant Topchyan,[2] Roberto Tateo,[3] and Ara Sedrakyan[2]

[1] *Grupo de Física Matemática da Universidade de Lisboa, Av. Prof. Gama Pinto 2, 1649-003 Lisboa, Portugal.*
[2] *Alikhanyan National Laboratory, Yerevan Physics Institute, Armenia*
[3] *Dipartimento di Fisica, Università di Torino, and INFN, Sezione di Torino, Via P. Giuria 1, I-10125 Torino, Italy*

(ΩDated: August 28, 2020)

Integer Quantum Hall plateau transitions are usually modeled by a system of non-interacting electrons moving in a random potential. The physics of the most relevant degrees of freedom, the edge states, is captured by a recently-proposed random network model, in which randomness is induced by a parameter-dependent modification of a regular network. In this paper we formulate a specific map from random potentials onto 2D discrete surfaces, which indicates that 2D gravity emerges in all quantum phase transitions characterized by the presence of edge states in a disordered environment. We also establish a connection between the parameter in the network model and the Fermi energy in the random potential.

Introduction. The investigation of plateau transitions in the Quantum Hall Effect (QHE) continues to be one of the most exciting research topic in modern condensed matter physics. Much of the current interest is motivated by the emergence of a similar type of physics in the context of topological insulators. The Quantum Hall plateau transition is in fact an example of a metal-insulator transition (see [1] for a review) with the plateau region between the Landau Levels (LLs) corresponding to the insulating phase where all the states are localized due to the external magnetic field. The transition is a disorder-induced localization/delocalization transition of Anderson type, characterized by a divergent localization length ξ at the critical point with localization index ν.

In this paper we focus on QHE plateau transitions, which are usually modelled by a system of non-interacting electrons moving in a 2D random potential (RP) $V(\mathbf{r})$ characterized by a white-noise Gaussian distribution. Throughout the paper, we shall consider RPs with a finite correlation length generated by N Gaussian sources, i.e.

$$V(\mathbf{r}) = \sum_{i=1}^{N} W_i \exp\left(-\frac{|\mathbf{r}-\mathbf{r}_i|^2}{2\sigma^2}\right), \qquad (1)$$

where σ^2 is the variance, $\mathbf{r}_i$ is the position vector of the $i-$th source and the coefficients $\{W_i\}_{i=1}^N$ are randomly chosen in $[-W, W]$, with $W \in \mathbb{R}$. In such RP landscape, electrons are localized [2] and fill the Fermi sea which actually consists of a collection of lakes with characteristic size l, as displayed in FIG. 1. The delocalization of electrons is triggered by the presence of an external magnetic field B which does not change the total energy of the system but rearranges the eigenstates and forms LLs. The mechanism of delocalization can be intuitively explained using the following semi-classical picture. At large B, the electrons in a LL are strongly localized and their state corresponds to an orbital motion with small radius $r \sim 1/B$. At the boundary of a lake, the orbital motion combines with the reflection due to the potential giving rise to a precession motion along equipotential lines (cycloid). The electrons localized along the boundaries of the lakes form the so-called edge states. When an edge electron approaches a saddle point that is sufficiently close to the boundaries of two neighbour lakes, quantum tunnelling of the particle from one boundary to the other becomes sizable (see FIG. 2). Therefore, edge electrons may either jump from one lake to another with a finite probability t, or continue to move along the boundary of the original lake with probability r, with $t^2 + r^2 = 1$. The presence of such quantum scattering nodes at saddle points enables electrons to reach arbitrary distances with a finite probability and is at the origin of the lo-

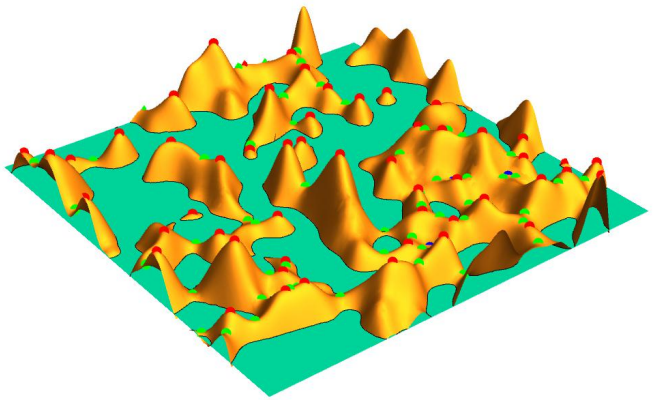

FIG. 1: RP generated by $N = 2500$ Gaussian sources on a torus. Points mark maxima (red), minima (blue) and saddle points (green). The plane denotes the Fermi level.

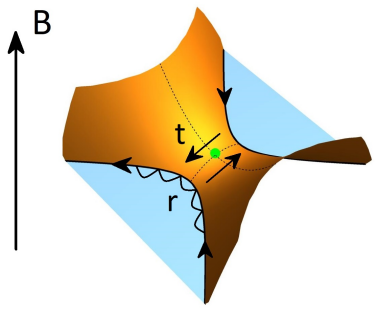

FIG. 2: Neighborhood of a saddle point (green dot) separating two lakes (blue areas) in a RP. The cycloid represents the motion of edge states along the boundary of a lake. The parameters r and t denote the reflection and transmission probabilities, respectively, while B is the magnetic field.

calization/delocalization transition. Taking inspiration from this semi-classical picture, J. Chalker and P. Coddington (CC) [3] formulated a network model of quantum scattering nodes based on a regular lattice that is meant to provide an effective description of the physics of edge states (the only relevant degrees of freedom in plateau transitions). Its generalization on a Kagome lattice was proposed in [4] and a similar network model for the Spin Quantum Hall Effect (SQHE) was studied in [5, 6]. Numerical investigations of the localization length ξ at the critical point, i.e. $\xi \sim (t-t_c)^{-\nu}$ with $t_c = 1/\sqrt{2}$, resulted in $\nu = 2.56 \pm 0.62$ for a regular lattice [7–9, 11, 12] and $\nu = 2.658 \pm 0.046$ for the Kagome lattice [4]. Both these values are not compatible with the experimental value $\nu = 2.38 \pm 0.06$ measured for plateau transitions in the IQHE [13, 14]. A possible solution to fix the discrepancy was put forward in [15, 16] by considering random networks (RNs), which should better account for the disorder present in a RP. The numerical estimate obtained in this framework $\nu = 2.372 \pm 0.017$ [15, 16] confirms indeed a very good agreement with the experimental result.

In [15, 16] it was also argued that the randomness of RNs leads to the appearance of 2D quantum gravity, in the continuum limit. The primary objective of this paper is to show that 2D gravity is indeed emerging from the RPs framework, establishing a precise correspondence between RNs and RPs. Notice that quantum gravity is also involved in the understanding of Fractional QHE [17, 18] revealing the physics of Laughlin wave-function. In that context, the interaction between fermions is responsible for the emergence of gravity in the bulk. Instead, in the present paper gravity is related to the 1+1 dimensional edge states, which originates from the RP.

Network models with geometric disorder. Let us briefly review the construction of RNs carried on in [15, 16]. The main idea is to generate randomness in a regular CC network making an extreme replacement, which consists in "opening" a scattering node in the horizontal (vertical) direction with probability p_0 (p_1) setting $t = 0$ ($t = 1$) (see FIG. 3), or leaving it unchanged with probability $1 - p_0 - p_1$. In the following, we shall set $p_n = p_0 = p_1$ to maintain statistical isotropy [15, 16]. Since in the RP picture the scattering node simulates a saddle point and the four squares surrounding it corresponds to an alternate sequence of maxima and minima (see FIG. 3), after the extreme replacement the scattering node becomes an hexagon containing a maximum (minimum) and two adjacent triangles each containing a minimum (maximum), as depicted in FIG. 3. Thus, starting from a regular

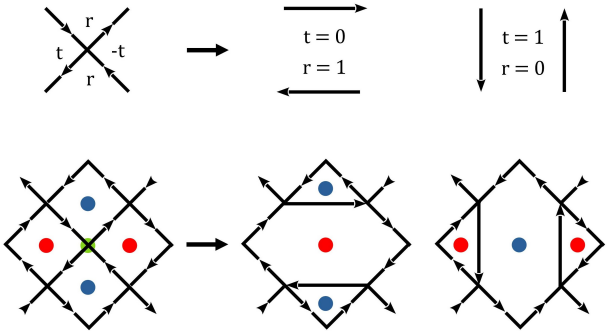

FIG. 3: Top: "opening" of a scattering node in the horizontal and vertical directions. Bottom: result of the extreme replacement on the network. Red, blue and green points mark maxima, minima and saddle points in the corresponding RP framework.

CC network where all the faces are quadrangles and randomly making the extreme replacement with probability p_n, a tiling of the plane with $n-$gons is obtained. In [16] it was shown that in this type of RNs the localization index has a non-trivial dependence on the replacement probability p_n, with a line of critical points for $p_n \in [0, 1/2]$. A natural question addressed in the present paper concerns the physical interpretation of the parameter p_n within the RP model. As we shall see, p_n is connected with the height or Fermi energy level of edge states in the RP landscape.

Random potentials and discrete surfaces. The RP (1) corresponds to a 2D smooth surface characterized by N_{max} maxima, N_{min} minima, N_{sp} saddle points (see FIG. 1) and with Euler characteristics

$$\chi = N_{min} + N_{max} - N_{sp} \,, \tag{2}$$

according to Morse theory [19]. Connecting maxima and minima following the gradient of $V(\mathbf{r})$ gives a unique quadrangulation of the surface, namely a 2D discrete surface S made of $v = N_{max} + N_{min}$ vertices, e edges and $f = N_{sp}$ quadrangular faces (see FIG. 4). Denoting by n_i the connectivity of the $i-$th vertex, i.e. the number of edges connected to it, the Euler characteristics

$\chi = v - e + f$ of S can be expressed as

$$2\pi\chi = \sum_{i=1}^{v} R(n_i) \,, \quad R(n) = \frac{\pi}{2}(4-n) \,, \tag{3}$$

where, according to Gauss-Bonnet theorem, $R(n)$ can be interpreted as the discrete Gaussian curvature associated to each vertex of S. Formula (3) follows immediately from the fact that $e = 2f = \frac{1}{2}\sum_{i=1}^{v} n_i$, from which $\chi = v - e + f = v - f = \frac{1}{4}\sum_{i=1}^{v}(4 - n_i)$.
Notice that by construction each face of S contains exactly one saddle point. Therefore, connecting saddle points belonging to nearest neighbor faces of S results in a dual 2D discrete surface S^*, made of $v^* = f$ vertices with connectivity 4, e^* edges and $f^* = v$ $n-$gonal faces, where n is the connectivity of the vertex of S lying within each face of S^* (see FIG. 4). By duality, each $n-$gonal face of S^* carries a discrete Gaussian curvature $R(n)$ and brings a local contribution to $2\pi\chi$ as described in eq. (3). Following this procedure, to each RP is associated a 2D random discrete surface S or equivalently S^*, which ultimately corresponds to a network model where either the connectivity of the sites or the number of sides of the faces carries the discrete Gaussian curvature of the surface. In the following, we will denote by S or S^* both the discrete surface or the network associated to it.

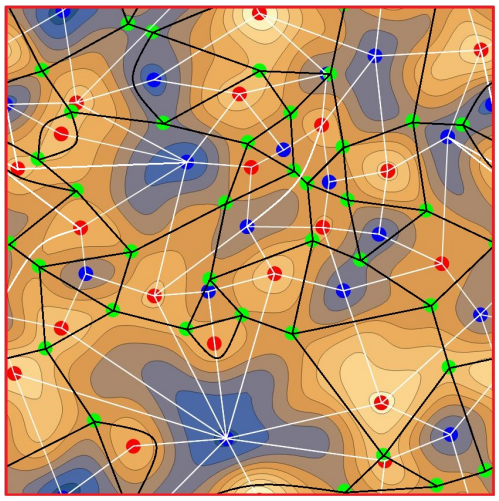

FIG. 4: Topography of a RP generated by $N = 900$ Gaussian sources placed on a torus. Points mark maxima (red), minima (blue) and saddle points (green). White and black lines are the edges of S and S^*, respectively.

Random potentials vs. Random networks. To establish contact between RPs and RNs, let us give a concrete example. Consider a RP generated by $N = L^2$ Gaussian sources evenly distributed on a regular square lattice of size L with unit spacing and doubly periodic boundary conditions, i.e. a torus. Let $\mathbf{r}_i = (x_i, y_i) = (i \mod (L), \lceil i/L \rceil)$ be the position of the $i-$th source on the lattice, where $\lceil * \rceil$ is the ceiling function. Then, the RP at the generic point $\mathbf{r} = (x, y) \in [0, L-1] \times [0, L-1]$ of the torus is

$$V(\mathbf{r}) = \sum_{i=1}^{N} \sum_{\mathbf{n}\in\mathbb{Z}^2} W_i \exp\left(-\frac{|\mathbf{r} - \mathbf{r}_i + \mathbf{n}L|^2}{2\sigma^2}\right) , \tag{4}$$

where the range of the summation index $\mathbf{n} = (n_x, n_y)$ is restricted to $\{-1, 0, 1\} \times \{-1, 0, 1\}$ in the numerical simulation. Eq. (2) implies that the critical points of (4) are such that $N_{max} + N_{min} = N_{sp}$ since $\chi = 0$ for a torus. In FIG. 6, the distributions of critical points per unit height of the potential are reported for a statistical sample consisting of $m = 45$ simulations on square lattices of size $L = 300$ with $W = 1/10$ and $\sigma = \sqrt{2}$. Since at finite W and σ the potential $V(\mathbf{r})$ is bounded, the distributions are defined on a finite support, also in the limit $L \to \infty$. However, in the case under consideration, they are well approximated by Gaussian distributions with expectation values $\mu_{max} = -\mu_{min} = 0.187$, $\mu_{sp} = 0$ and standard deviations $\sigma_{max} = \sigma_{min} = \sigma_{sp} = 0.119$. Following the procedure described in the previous section, a discrete surface S or equivalently S^* can be uniquely associated to (4) (see FIG. 4). The introduction of a Fermi level $c \in \mathbb{R}$ induces a truncation of both S and S^* since a fraction of the vertices stays inside the Fermi lakes. The resulting truncated surface S_c or S_c^* is such that the disconnected portions of the original surface lying under the Fermi level, which may contain an arbitrary number of vertices, can be replaced with single isolated vertices as displayed in FIG. 5. This operation is indeed physically meaningful since the scattering of edge states is not affected by the bulk of Fermi lakes. Therefore, varying the Fermi level produces a flow within the space of discrete surfaces parametrized by c.

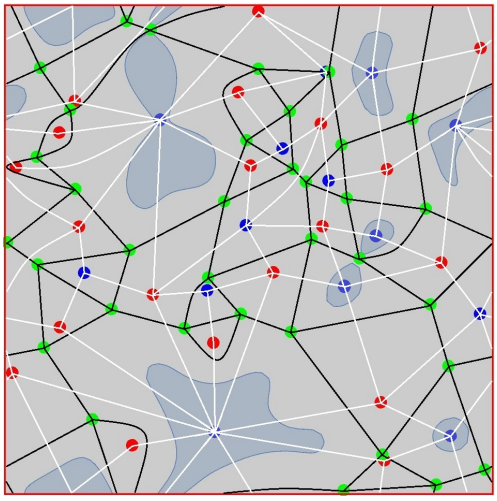

FIG. 5: Networks associated to the truncated discrete surfaces S_c and S_c^*. White and black lines are the links of S_c and S_c^*, respectively, while the areas highlighted in light blue correspond to the regions under the Fermi level.

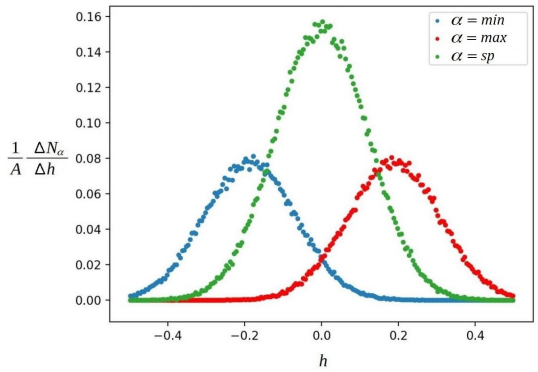

FIG. 6: Number of maxima (ΔN_{max}), minima (ΔN_{min}) and saddle points (ΔN_{sp}) in the height range $[h, h+\Delta h]$, with $\Delta h = 1/200$, divided by the area A of the lattice. The statistical sample consists of $m = 45$ simulations on square lattices of size $L = 300$, i.e. $A = mL^2$, with $W = 1/10$ and $\sigma = \sqrt{2}$.

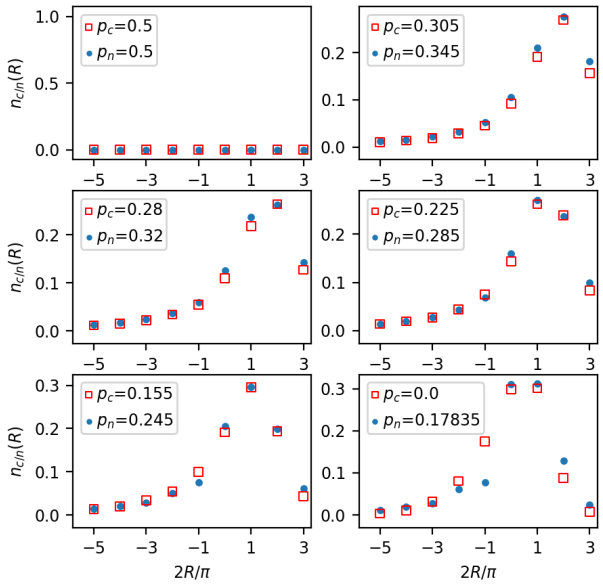

FIG. 7: Curvature distributions for the RN (blue dots) and the dual network S_c^* (red squares) for various values of the parameters p_n and p_c which minimize the SSE.

Observe that the truncation of the discrete surfaces caused by the Fermi level corresponds to the removal of sites in the associated networks and, consequently, to the emergence of polygonal faces with a larger number of sides (see FIG. 5). The net effect of this process is very reminiscent of that induced in the CC network by the surgery performed in [15, 16] leading to RNs. For this reason, we expect the replacement probability p_n of RNs to be somehow related to the Fermi level in RPs.

For the purposes of comparing these two models, it is first necessary to restore particle-hole duality in the RP framework since RNs, which tend to Dirac fermion models in the continuum limit, possess it. To this aim, the range of energies accessible to fermions in the RP is restricted from $[c, +\infty[$ to the symmetric interval $[-|c|, |c|]$ and the complementary interval $[-\infty, -|c|] \cup [|c|, +\infty[$ is labelled as "non-valid" region.

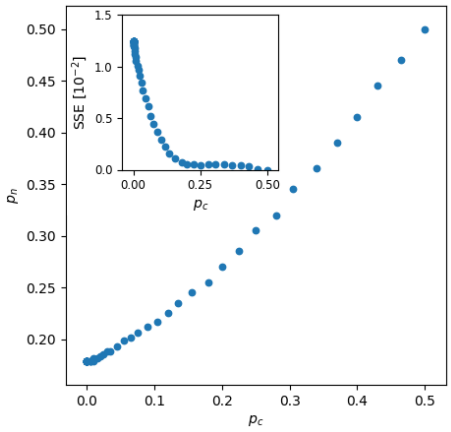

FIG. 8: Correspondence between the replacement probability p_n and p_c obtained searching for the best match between the two curvature distributions. The inset plot gives the estimated SSE as a function of p_c.

Secondly, notice that the replacement probability p_n in the RN framework is equivalent to half the ratio between the number of removed scattering nodes, i.e. saddle points, and the total number of them. This observation suggests that half of the ratio between the number of saddle points in the non-valid region and the total number of them, denoted by p_c, is the most appropriate parameter of the RP to be put in relation to p_n. In this respect, the observable taken into consideration is the distribution of discrete Gaussian curvatures R of the polygons tiling both the RN and the dual network S_c^* to varying of p_n and p_c, respectively. Denoting by $n_n(R)$ and $n_c(R)$ the number of polygons with curvature R in the RN and in S_c^*, respectively, the defining criterion for the association between p_n and p_c is the minimization of the sum of squared errors, $SSE = \sum_{R\in\mathbb{N}} (n_n(R) - n_c(R))^2$. In FIG. 7 distributions of curvatures in both the RN and S_c^* are compared for some values of p_n and p_c that minimize the SSE. The statistical samples consist of more than 50 RN simulations on a 100×1000 network for each value of $p_n \in [0, 1/2]$ and 45 RP simulations on a square lattice of size $L = 300$ for each value of $c \in [0, 1/2]$. A good agreement between the two models is obtained for a suitable correspondence $p_n \leftrightarrow p_c$, as reported in FIG. 8.

Conclusions. There are strong evidences that the field-theory description of plateau transitions corresponds to a model of fermions interacting with random gauge and scalar potentials and also with structurally-disordered geometry. Indicating that, in the scaling limit, localization transitions of this type are correctly described by matter fields coupled to 2D quantum gravity. Starting from a

random potential model, we have explicitly constructed a map onto the 2D disordered graphs S_c and S_c^* depending on the Fermi-level. Thus, observing the appearance of the basic ingredient of random network models [15, 16] for Quantum Hall plateau transitions and giving an interpretation of the replacement probability in term of the Fermi energy. S_c and S_c^*, being quadrangulations and $n-$gon tiling's of the plane, have a straightforward interpretation as discrete random surfaces, explicitly showing the emergence of 2D gravity. As discussed also in [15], the notion of functional measure of random surfaces remains an open problem. From the current analysis, it appears that the distribution of Gaussian curvatures on the random surface associated with the random potential coincides with the corresponding distribution in the random network model, suggesting that the functional measure of random surfaces can be defined in terms of the measure of random potentials. In conclusion, we revealed a deep link between random potentials in Anderson localization problem and 2D curved surfaces, where the edge states responsible for plateau transitions live.

Acknowledgments. A.S. acknowledge University of Turin and INFN for hospitality and ARC grant 18T-1C153 for financial support. This work was also partially supported by the INFN project SFT and by the FCT Project PTDC/MAT-PUR/30234/2017 "Irregular connections on algebraic curves and Quantum Field Theory".

[1] B. Huckestein, Rev. Mod. Phys. 67, 357 (1995).
[2] E. Abrahams, P. W. Anderson, D. C. Licciardello, and T. V. Ramakrishnan, Phys. Rev. Lett. 42, 673 (1979).
[3] J. T. Chalker and P. D. Coddington, J. Phys. C 21, 2665 (1988).
[4] N. Charles, I. Gruzberg, A. Klümper, W. Nudding, and A. Sedrakyan, arXiv:2003.08167.
[5] V. Kagalovsky, B. Horovitz, Y. Avishai, and J. T. Chalker, Phys. Rev. Lett. 82, 3516 (1999).
[6] I. A. Gruzberg, A. W. W. Ludwig, and N. Read, Phys. Rev. Lett.82, 4524 (1999).
[7] K. Slevin and T. Ohtsuki, Phys. Rev. B 80, 041304(R) (2009).
[8] M. Amado, A. V. Malyshev, A. Sedrakyan, and F. Domnguez- Adame, Phys. Rev. Lett. 107, 066402 (2011).
[9] H. Obuse, I. A. Gruzberg, and F. Evers, Phys. Rev. Lett. 109, 206804 (2012).
[10] K. Slevin and T. Ohtsuki, Int. J. Mod. Phys. Conf. Ser. 11, 60 (2012).
[11] W. Nuding, A. Klümper, and A. Sedrakyan, Phys. Rev. B 91, 115107 (2015).
[12] J. P. Dahlhaus, J. M. Edge, J. Tworzydo, and C. W. J.Beenakker, Phys. Rev. B 84, 115133 (2011).
[13] W. Li, G. A. Csăthy, D. C. Tsui, L. N. Pfeiffer, and K. W. West, Phys. Rev. Lett. 94, 206807 (2005).
[14] W. Li, C. L. Vicente, J. S. Xia, W. Pan, D. C. Tsui, L. N. Pfeiffer, and K. W. West, Phys. Rev. Lett. 102, 216801 (2009).
[15] I. A. Gruzberg, A. Klümper, W. Nuding, and A. Sedrakyan, Phys. Rev. B, 95, 125414 (2017).
[16] A. Klümper, W. Nuding, and A. Sedrakyan, Phys. Rev. B 100, 140201(R) (2019).
[17] F. D.M. Haldane, Phys.Rev.Lett.107, 116801 (2011).
[18] T. Can, M. Laskin, P. B. Wiegmann, Annals of Physics 362 (2015) 752794.
[19] J. Milnor, Morse Theory-Princeton University Press, Pinceton, New Jersey 1963.